

## **DYNAMIC ANALYSIS OF HEAP LEACH PAD UNDER HIGH PHREATIC LEVELS**

By: Jorge Castillo<sup>1</sup>, Dave Hallman<sup>2</sup>, Peter Byrne<sup>3</sup>, Denys Parra<sup>4</sup>.

### **SUMMARY**

The occurrence of high phreatic levels is not common in heap leach pads. However some sulfide copper heaps, where the acid solution used for leaching degrades the ore, can result in the occurrence of relatively high phreatic levels. This condition can compromise stability of the leaching facility, particularly in active seismic zones where high magnitude earthquakes could induce liquefaction of the saturated ore and cause a flow failure of the heap.

This paper presents a dynamic analysis of heap leach pad stability under high phreatic levels and various levels of seismic loading. The dynamic analyses were conducted as fully non-linear two dimensional analyses with fully coupled liquefaction triggering using the Fast Lagrangian Analysis of Continua (FLAC) computer code. The potentially liquefiable zones were modeled considering an elasto-plastic formulation implemented in the user defined UBCSAND model, which is a state-of-art procedure.

The geotechnical parameters, appropriate earthquake record selection and modification, model calibration, numerical analyses and results are discussed in the following sections.

### **1.0 INTRODUCTION**

Heap leach design is typically based on the assumption that the phreatic level should not be higher than 1 meter during normal operating conditions. The phreatic level within the heap is controlled mainly by the solution collection system sizing and ore permeability. However, with sulfide copper ore, the acid solution used for leaching progressively degrades the ore, and the occurrence of relatively high phreatic levels is more common, often much more than 1 meter. This condition can compromise the stability of the heap leach facility particularly in active seismic zones, where high magnitude earthquakes can induce liquefaction of the saturated ore and a flow failure of the heap.

---

<sup>1</sup> Senior Geotechnical Engineer, Vector Colorado LLC, [castillo@vectoreng.com](mailto:castillo@vectoreng.com)

<sup>2</sup> Senior Geotechnical Engineer, Principal, Vector Colorado LLC, [hallman@vectoreng.com](mailto:hallman@vectoreng.com)

<sup>3</sup> Professor Emeritus at the University of British Columbia, [pmb@civil.ubc.ca](mailto:pmb@civil.ubc.ca)

<sup>4</sup> Engineering Manager, Vector Perú S.A.C., [parra@vectoreng.com](mailto:parra@vectoreng.com)

Typically, the ore placed in the leach pad could be ROM ore or crushed ore, classified as sandy gravel to gravelly sand. The fines content (percent by weight finer than 0.074 mm or a No. 200 sieve) often ranges between 15 to 35 percent and classifies as low plasticity silt. Most of the heap leach pads in Peru are located in valleys which require the use of a berm at the toe of the heap to enhance stability.

This paper presents the stress-strain static and dynamic stability analyses of a typical copper heap leach pad, with characteristics common to most of the valley fill leach pad facilities in Peru.

The dynamic analyses were conducted as fully non-linear elasto-plastic two-dimensional analyses with fully coupled liquefaction triggering using the Fast Lagrangian Analysis of Continua (FLAC) finite difference code (Itasca, 2004). The FLAC code solves the equations of motion in explicit form in the time domain using very small time steps and incorporates the non-linear inelastic stress-strain soil behavior.

The potential liquefaction zones were modeled considering the elasto-plastic formulation implemented in the UBCSAND model which is a user defined model incorporated into the 2D FLAC version (Itasca, 2004). The UBCSAND model was developed by Professor Peter M. Byrne and his colleagues at the University of British Columbia (Byrne, 2003 and 2005). The UBCSAND model simulates the stress-strain behavior of soil under static or cyclic loading for drained or un-drained conditions by using an elastic-plastic formulation, where the shear modulus has both elastic and plastic components.

Typical state-of-practice procedures for evaluating liquefaction use separate analyses for liquefaction triggering, displacement, and flow slides and cannot predict generation of excess pore-water pressure, accelerations, and displacement patterns simultaneously. The UBCSAND model, which is a state-of-art procedure, involves dynamic difference analysis using effective stress procedures coupled with fluid flow enabling the pore pressures, accelerations and displacements caused by a specific input motion to be estimated. In this manner liquefaction triggering, displacement and flow slide potential are addressed in a single analysis.

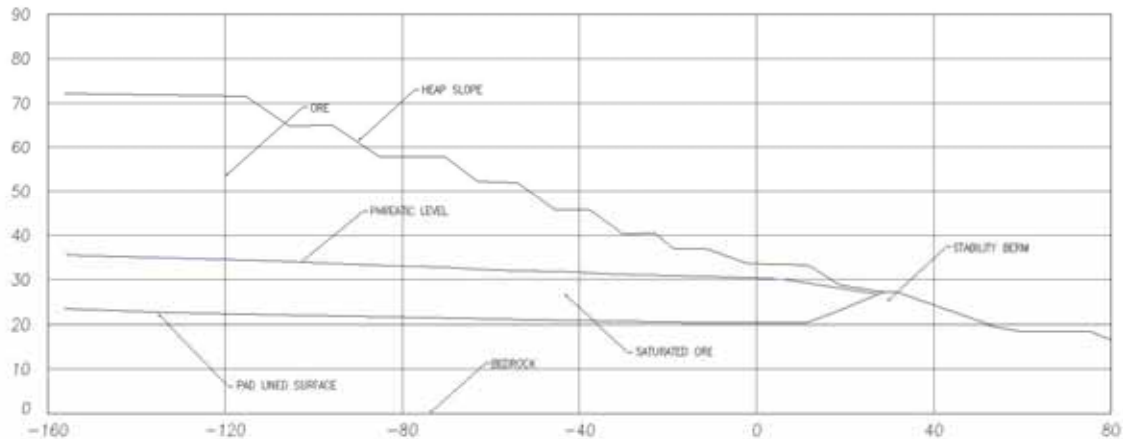
The stability analyses steps which are described in this paper include:

- 1) Static analysis to establish the state of stress prior to earthquake loading;
- 2) Selection of earthquake time-history records and their modification to obtain a better match to the design spectra;
- 3) Model calibration based on cyclic triaxial tests and field test results;

- 4) Fully coupled non-linear dynamic liquefaction and deformation analysis considering state-of-art procedures; and
- 5) Discussion of results.

The analyses considered the typical heap cross section shown in Figure 1.

**Figure 1: Geometry Modeled**



## 2.0 STATIC ANALYSIS

Static analyses were conducted using the FLAC code primarily to establish the state of stress prior to earthquake loading. The heap leach pad ore properties were modeled using the UBCSAND model. The elastic and plastic shear and bulk modulus are computed as functions of  $(N_1)_{60}$  values (see section 3.3 for values adopted). The material properties utilized are based on the values obtained from laboratory testing, published literature and previous experience with similar materials. The parameters adopted for the static analysis are given in Table 1.

**Table 1: Material Properties**

Material	Density		Elastic Properties		Mohr-Coulomb	
	KN/m <sup>3</sup>	kg/m <sup>3</sup>	Bulk Modulus (MPa)	Shear Modulus (MPa)	Cohesion (KPa)	Friction angle
Ore	16.0	1633	45.0	15.0	5	36

The initial state of stress was established by reaching mechanical and seepage flow steady state equilibrium prior to applying the seismic loading. This initial static shear stress distribution is very important, because it can have a large affect on liquefaction triggering.

### **3.0 DYNAMIC ANALYSIS**

The dynamic analysis was performed considering the fully non-linear method with the FLAC code (Itasca, 2004). The UBCSAND model was incorporated into the 2D FLAC version by modifying the existing Mohr-Coulomb model. The dynamic liquefaction analyses were also checked against the possibility for a flow slide to develop in a typical state-of-practice post-liquefaction residual strength analysis. In these analyses checks, the shear strength for model elements that were indicated to have liquefied were changed to residual strength and the static stability checked to see if the conditions for massive uncontrolled movement or flow sliding were reached, i.e. a static factor of safety less than 1.0 using residual strength.

#### **3.1 Earthquake Input Motion**

For the dynamic analysis one or more earthquake time-histories that correspond to the design ground motions are required for the model input ground motion. The record(s) should be selected on the basis of the magnitude of the event (i.e. duration), tectonic setting (subduction zone thrust faulting versus shallow crustal), source-to-site distance, frequency content, and local site conditions.

An acceleration time-history was selected from historic earthquake records consistent with the level of shaking for the 500 year return period with 0.35g peak horizontal acceleration at a rock site station. The peak ground acceleration represents a typical value for the western slope of the Peruvian Andes Mountains as shown in previous regional seismic hazard studies (Castillo and Alva, 1993; Sharma and Candia-Gallegos, 1992). Table 2 summarizes the key characteristics of the original October 3, 1974 Lima Mw = 8.1 earthquake, Parque de la Reserva station, East-West component record adopted for use in the analysis.

The acceleration time history was modified in the frequency domain to obtain a better match to the design spectra. Figure 2 presents a plot of the modified record used in the analysis. Figure 3 presents a plot of the 5 percent of critical damping acceleration response spectra for the modified record compared with the design spectra as well as the Peruvian Building Code spectra. As shown in Figure 3 the matching procedure results in a modified record spectrum that matches the design spectra over a much wider range of frequencies than normally observed. Although providing a better match to the design spectra, this procedure also means that more periods are subject to the full design acceleration level rather than the peaks and troughs observed in the natural record. This will tend to give exaggerated estimates of energy input and displacement demand (Finn, 2000) and yield conservative results.

Additionally the record modified to match the 500 year return period ground motions was scaled to 0.20g and 0.15g to represent 100 and 50 year return period motions,

respectively. This is conservative for these shorter return periods since the large magnitude earthquake and source mechanism related to the 500 year return period hazard level are also being considered for these two shorter return periods.

**Figure 2: Modified Time History Records used for dynamic analysis**

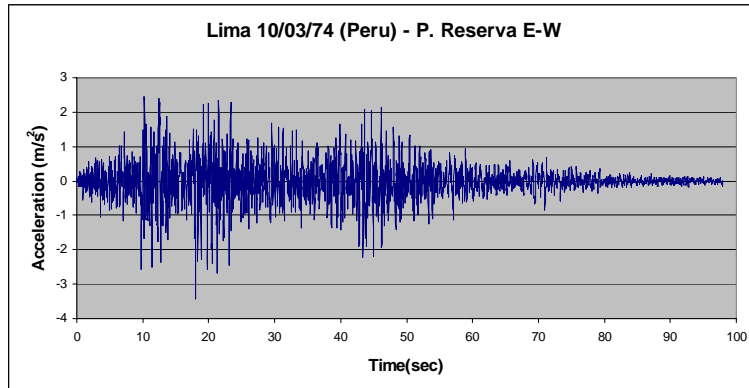
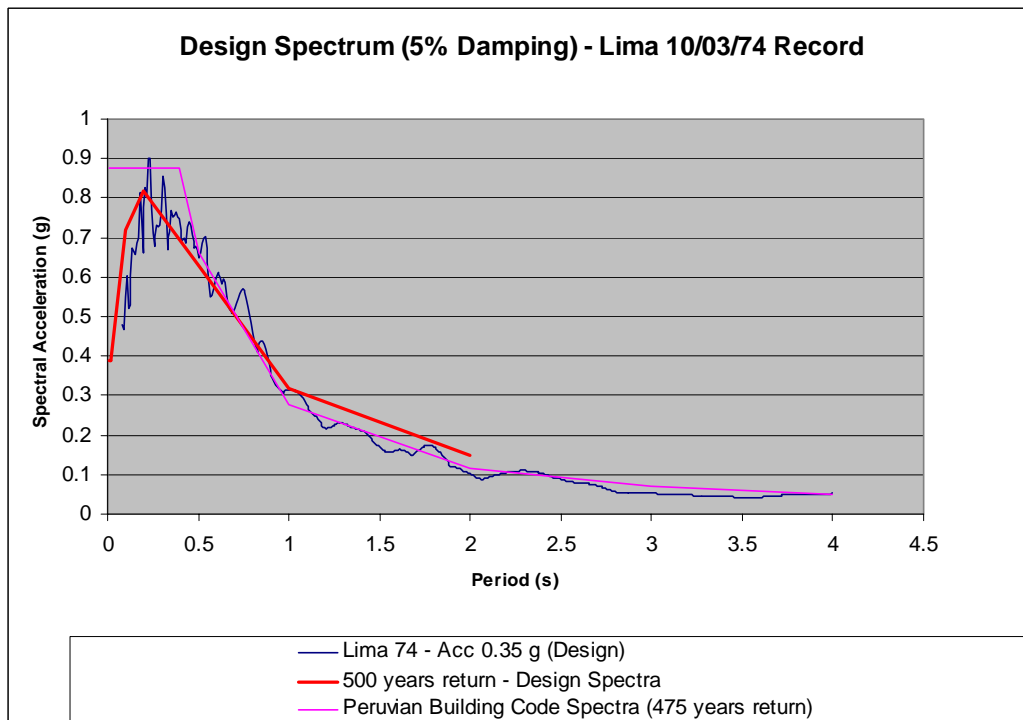


**Table 2 – Original Earthquake Time-History Records**

Earthquake	Magnitude (Mw)	Depth (Km)	Station	Comp.	Peak Ground Acceleration (m/s <sup>2</sup> )
Lima 10/03/74 (Peru)	8.1	21	Parque de la Reserva	E-W	1.92

**Figure 3: Design Spectrum versus Modified Time-History Record**

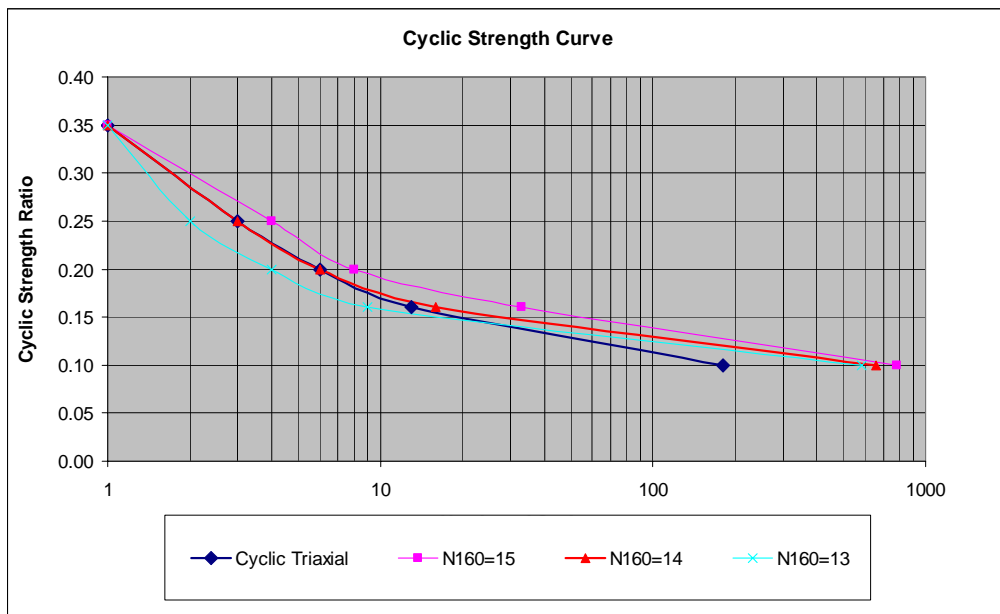


### 3.3 Model Calibration

The UBCSAND model implementation in FLAC was calibrated by selecting the  $(N_1)_{60}$  value that matches the results of cyclic triaxial testing performed on typical ore samples. The model calibration was accomplished by using a single element simulation in FLAC to model the laboratory tests. The single element was assigned an  $(N_1)_{60}$  value, friction angle and maximum shear modulus in accordance with the values presented in Table 1. Based on a comparison of the predicted number of cycles to liquefaction and the measured number in the laboratory test, the  $(N_1)_{60}$  was adjusted if necessary and the simulation repeated until the predicted and measured number of cycles were approximately the same.

A summary of the cyclic triaxial test and the UBCSAND calibration are shown in Figure 4. The data for the ore tested in this instance has a steeper cyclic stress ratio (CSR) vs number of cycles to liquefaction than test data for natural and mine tailings sand that were used to develop the UBCSAND model. Typically liquefaction is triggered by one or two big pulses during earthquake loading and the UBCSAND calibration should be fit to the test data in the lower load cycle region accordingly. As shown in Figure 4,  $(N_1)_{60} = 14$  fits the actual triaxial test data quite well for 10 cycles of loading or less. The model was also calibrated using results from simple shear CSR testing, which is less than cyclic triaxial. For the simple shear CSR results  $(N_1)_{60} = 9$  provides the best UBCSAND calibration, and was selected as the conservative  $(N_1)_{60}$  value for use in the model.

**Figure 4: Predicted and Measured Liquefaction Response for Typically Crushed Ore**



The  $(N_1)_{60}$  data obtained from SPT field values corrected for fines content range from 8 to 17 and with some specific zones averaging 20 blows per foot.  $(N_1)_{60}$  values between 8 and 14 are representative values, based on the field SPT distribution and density for the heap that was analyzed. This is consistent with the UBCSAND calibration from cyclic triaxial and simple shear testing of the ore.

Based on the laboratory and field testing results  $(N_1)_{60}=10$  was assumed as representative of the lower pad zone where the heap ore is saturated. Zero water bulk modulus was used for the upper pad zone where the ore in the heap is dry, consequently no excess pore water pressure was generated in this upper zone

### **3.4 Cases Analyzed**

Three (3) cases were modeled based on typical configuration and input motion considered. The analyses included the beneficial effect of the stability berm. In areas which do not include a stability berm dynamic deformations could be significantly higher than indicated. The analyses did not include any further remediation models beyond the existing stability berm. The cases analyzed included:

- CASE A: Current configuration, Lima 1974 input motion modified for 500 years return period design spectra.
- CASE B: Current configuration, Lima 1974 input motion from Case A scaled to 100 years return period peak ground acceleration.
- CASE C: Current configuration, Lima 1974 input motion from Case A scaled to 50 years return period peak ground acceleration.

### **3.5 Results**

The results of this study were divided into three parts corresponding to ground motion return periods of 500, 100 and 50 years. The seismic response results for 500 year returns for the modified Lima 1974 earthquake Parque de la Reserva record are shown in Appendix A, Figures A-1 to A-8 (Case A). The seismic response results for 100 year return period ground motion using a scaled version of the modified Lima 1974 earthquake record are shown in Appendix B, Figures B-1 to B-6 (Cases B). The seismic response results for 50 year return period ground motion using a scaled version of the modified Lima 1974 earthquake record are shown in Appendix C Figures C-1 to C-4 (Case C). Tables 3 summarize the heap leach pad dynamic analyses cases considered and their results.

**Table 3: Summary of Embankment Seismic Response**

Return Period (years)	Case	Earthquake Record	Geometry	Maximum Displacement (m)		Flow slide
				Horizontal	Vertical	
500	A	Lima 74	Current	3.5	1.0	yes
100	B	Lima 74	Current	2.0	0.5	yes
50	C	Lima 74	Current	0.7	0.2	No

Displacements at the conclusion of earthquake. Continued post-earthquake displacements were considered in a qualitative sense of whether or not a flow slide was likely to occur.

### 3.5.1 Case A: 500 year return period

The predicted dynamic behavior of the heap for the Lima 1974 earthquake Parque de la Reserva E-W record, which was modified to match the 500 year return period response spectrum, indicates maximum horizontal and vertical displacements of 3.5 m and 1 m, respectfully, as shown in Figures A-1 and A-2. Displacement of the model mesh at the conclusion of the earthquake loading is shown in Figures A-3 and A-4. These results do not consider any post-earthquake displacements that occur if the strength should drop to its residual value.

The deformed geometry resulting from the earthquake induced displacements was checked for the possibility of continued uncontrolled mass movements, i.e. a flow slide. The shear strength for elements indicated to have liquefied in the FLAC model were reduced to residual strength at the conclusion of the earthquake. The residual strength was expressed as a ratio of effective overburden pressure,  $S_u/p' = 0.15$  based on the  $(N_1)_{60}$  data. FLAC was then used to re-compute equilibrium. If very large additional deformations were needed to obtain equilibrium, or equilibrium could not be obtained for the post-earthquake geometry under static load, then a flow slide is indicated. These analyses indicate a large flow slide would occur as depicted in Figures A-5 and A-6. Although these figures indicate a failure mass overtopping the toe berm, the model mesh becomes too distorted to continue the computations and provide an estimate of the ultimate run out distance.

Predicted peak ground accelerations and excess pore water pressure in the heap toe area are shown in Figures A-7 and A-8. Decoupling of the heap response from the input motion as a result of liquefaction of the saturated base layer is clearly evident in the results as shown in Figure A-7.

### 3.5.2 Case B: 100 years return period

The predicted dynamic behavior of the heap for the modified Lima 1974 earthquake Parque de la Reserva record scaled to match the 100 year return period pga indicates

maximum horizontal and vertical displacements of 2.0 m and 0.5 m, respectfully, as shown in Figures B-1 and B-2. Displacement of the model mesh at the conclusion of the earthquake loading for these two cases is shown in Figures B-3 and B-4.

Due to the large displacements predicted to occur during the seismic loading, the resulting geometry was checked for the possibility of a flow slide. Again the shear strength for elements indicated to have liquefied were reduced to residual strength at the conclusion of the earthquake and the resulting post-earthquake geometry checked for large additional deformations under static load. These analyses indicate a flow slide overtopping the perimeter berm B as depicted in Figures B-5 and B-6. Although the model mesh becomes too distorted to continue the computations and provide an estimate of the ultimate run out distance these figures indicate the failure mass overtopping the toe berm is smaller than predicted for the 500 year return period ground motion.

### **3.5.3 Case C: 50 years return period**

Analysis of the heap for the modified Lima 1974 earthquake Parque de la Reserva record scaled to match the 50 year return period pga indicates maximum horizontal and vertical displacements of 0.70 m and 0.2 m respectively, as shown in Figures C-1 and C-2. Displacement of the model mesh at the conclusion of the earthquake loading is shown in Figures C-3 and C-4. The stability with residual strength values in zones predicted to liquefy was verified. In this case the displacements are small enough that no flow slide is indicated.

## **CONCLUSIONS**

The predicted dynamic behaviour of the heap leach pad analyzed for the 1974 Lima earthquake Parque de la Reserva record, modified to 500 years return period response spectrum, indicates that liquefaction occurs in the saturated zone of the heap producing large displacement of about 3.5 m. A large flow slide of material overtopping the toe berm was then predicted to occur. For ground motions scaled to match the 100 year return period pga, liquefaction triggering and a flow slide is also predicted to occur, although the amount of material that would overtop the toe berm is smaller than predicted for the 500 year return period ground motion. For ground motions scaled to match the 50 year return period pga the displacements are smaller and no flow slide is predicted to occur..

These results indicate that an adequate drainage system needs to be designed and constructed in order to minimize the phreatic surface in the heap in order to avoid pore-water pressure build-up at the toe of the heap and the resultant stability problems that could occur under seismic loading. Proper design of the drainage system should

include the possible affects of degradation of the ore due to the leachate being applied to the heap.

## REFERENCES

- Byrne, P. M. (2005). Professor Emeritus at the University of British Columbia, Civil Engineering Department. Personal communication.
- Byrne, P.M., S.S. Park and Beaty M.(2003) "Seismic liquefaction: centrifuge and numerical modeling". FLAC and Numerical Modelling in Geomechanics-2003. Proceeding of the 3<sup>rd</sup> International FLAC Symposium, Sudbury, Ontario, Canada pp 321-331, R. Brummer et al.(eds). Lisse: Balkema.
- Castillo J, and Alva J. (1993). "Peligro Sismico en el Peru", VII Congreso Nacional de Mecanica de Suelos e Ingenieria de Cimentaciones. Lima – Peru.
- Finn, W.D.L., 2000; "State-of-the-Art of Geotechnical Earthquake Engineering Practice", Soil Dynamics and Earthquake Engineering, Vol. 20, pp. 1 – 15.
- Itasca (2004). "Fast Lagrangian Analysis of Continua", Version 5.0. Itasca Consulting Group, Inc.
- Olson, M. and Stark, T. (2002). "Liquefied Strength Ratio from Liquefaction Flow Failure Case Histories". Canadian Geotechnical Journal, Vol. 39, pp. 629-647.
- Seed, H.B., Tokimatsu, K., Harder L. F., and Chung, R. M. (1984). "The Influence of SPT Procedures in Soil Liquefaction Resistance Evaluations". Report No. EERC 84-15, University of California, Berkeley.
- Sharma S, and M. Candia Gallegos. (1992). "Seismic Hazard Analysis of Peru". Engineering Geology, 32 73-79.
- Stark, T. and Mesri, G. (1992) "Undrained Shear Strength of Liquefied Sands for Stability Analysis", Journal of Geotechnical Engineering. Vol. 118, N° 11, pp. 1727-1747.
- Youd, T. et al. (2001). "Liquefaction Resistance of Soils: Summary Report from the 1996 NCEER and 1198 NCEER/NSF Workshops on Evaluation of Liquefaction Resistance of Soils". Journal of Geotechnical and Geoenvironmental Engineering, ASCE, October, pp.817-833.

**APPENDIX A – 500 YEARS RETURN PERIOD**

**FIGURE A-1: Horizontal Displacement Contours – Lima 74**

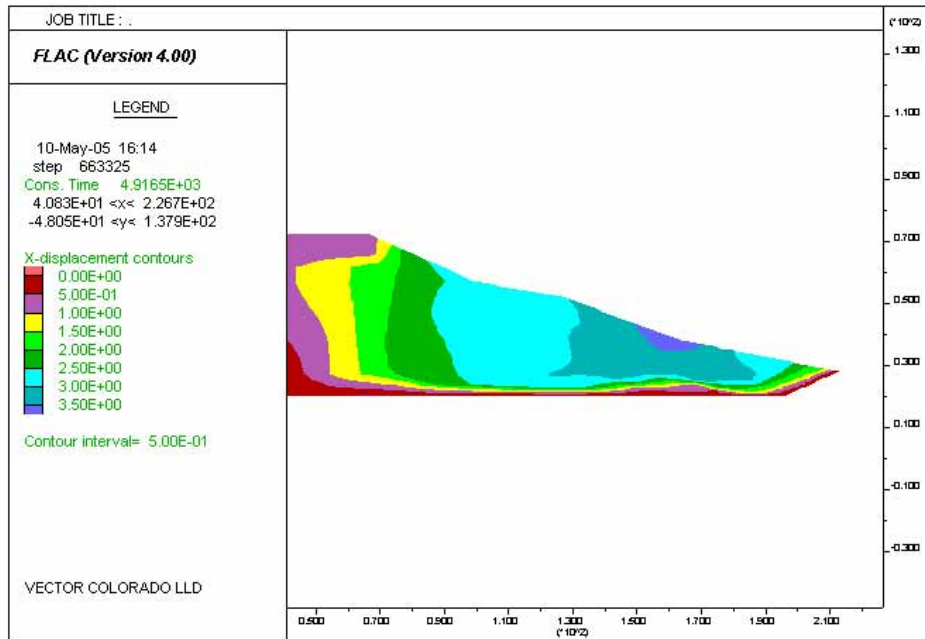


**FIGURE A-2: Vertical Displacement Contours – Lima 74**

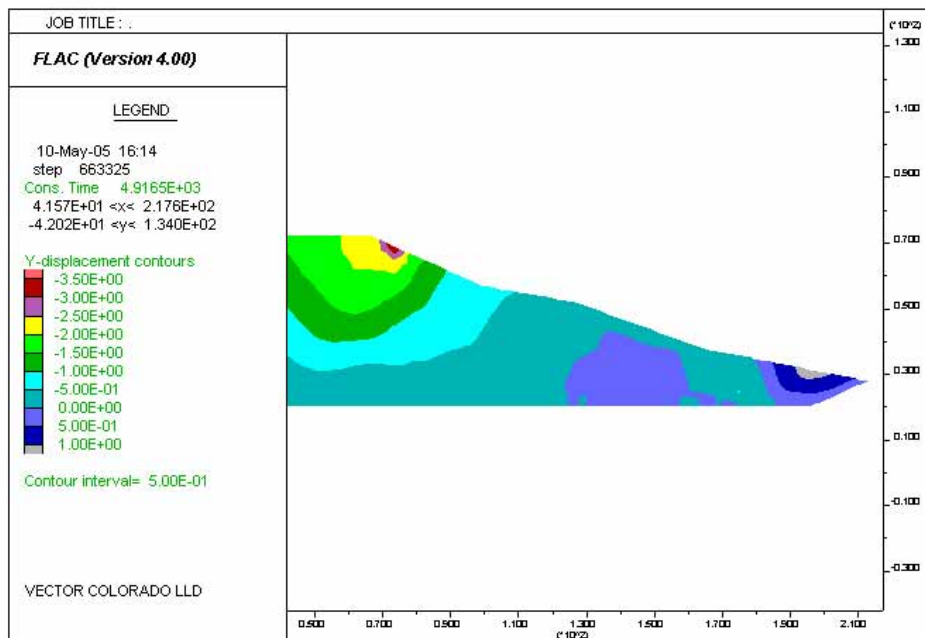


FIGURE A-3: Displacement (97 sec) – Lima 74

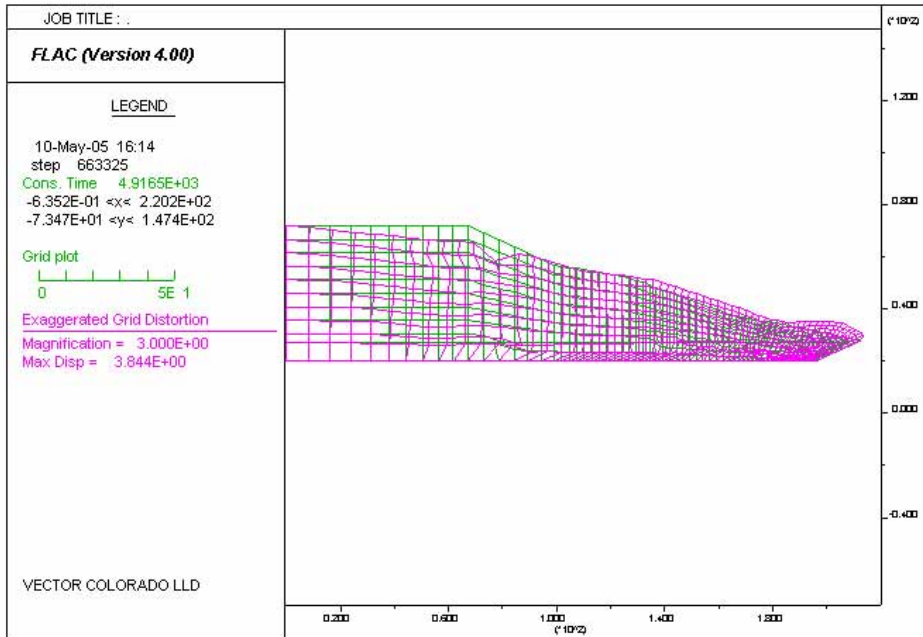


FIGURE A-4: SAME AS Fig 3 – zoom – Lima 74

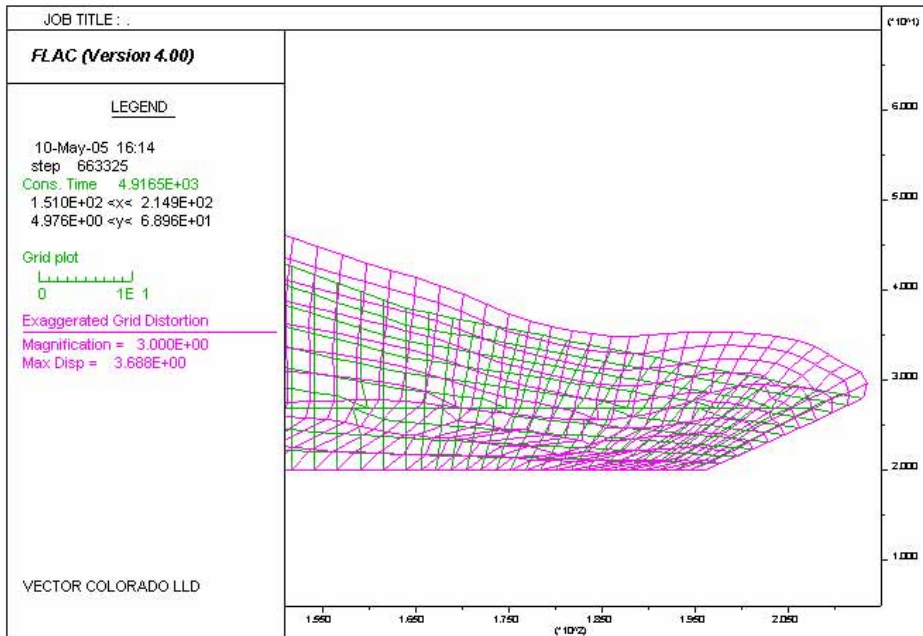


FIGURE A-5: Displacement  $S_u/p'=0.15$  – Lima 74

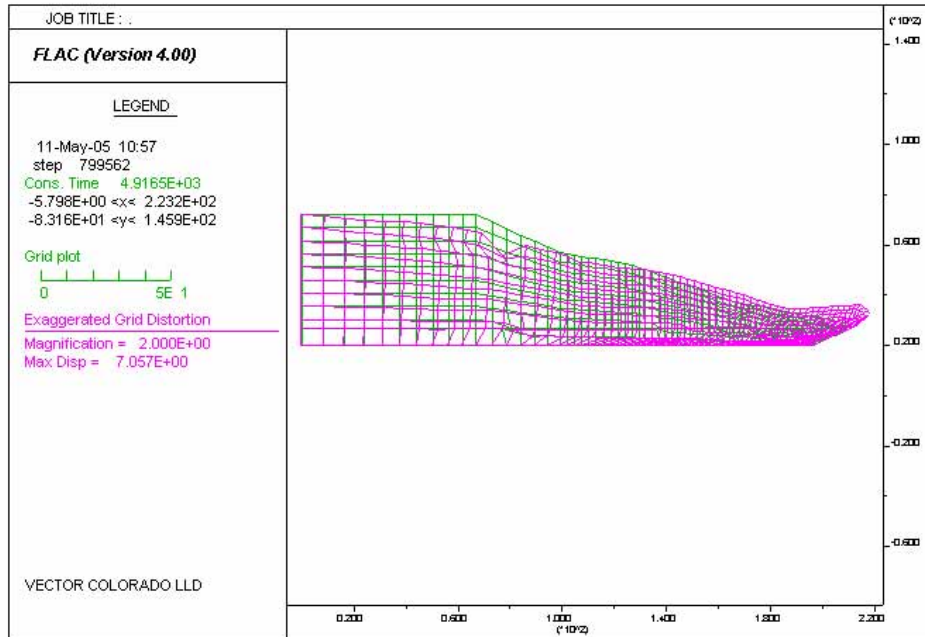


FIGURE A-6: Same as Figure A-5 – zoom – Lima 74

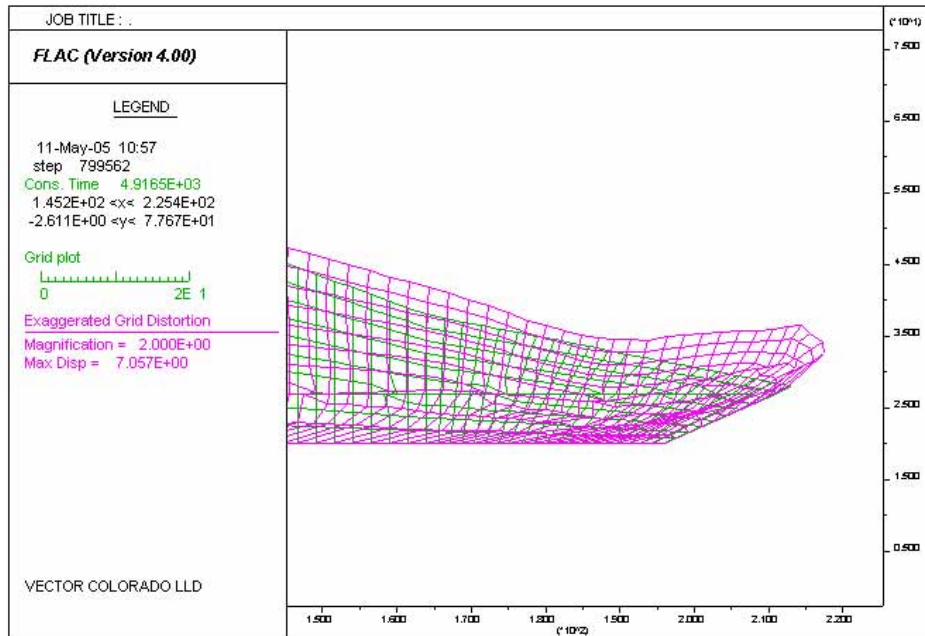


FIGURE A-7: Peak Acceleration at toe zone

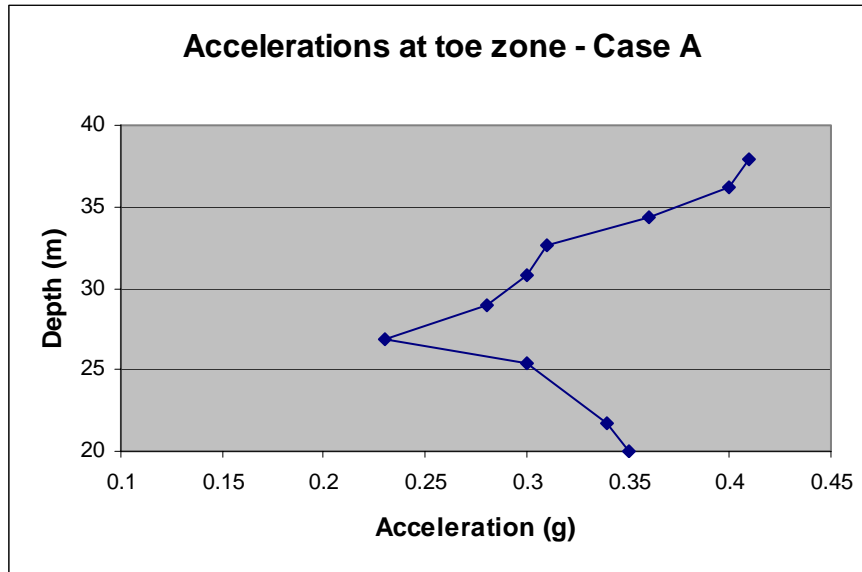
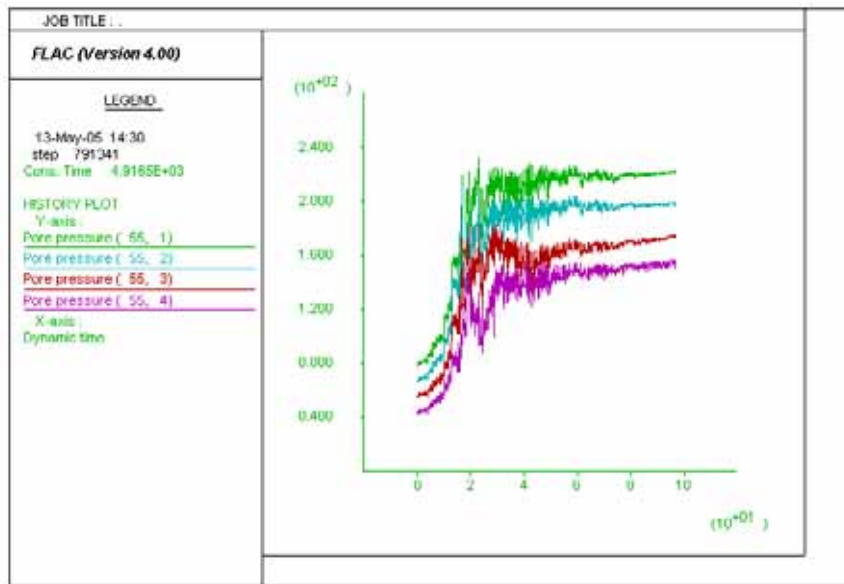


FIGURE A-8: Pore Pressure at toe zone



**APPENDIX B – 100 YEARS RETURN PERIOD**

FIGURE B-1: Horizontal Displacement Contours – Current geometry

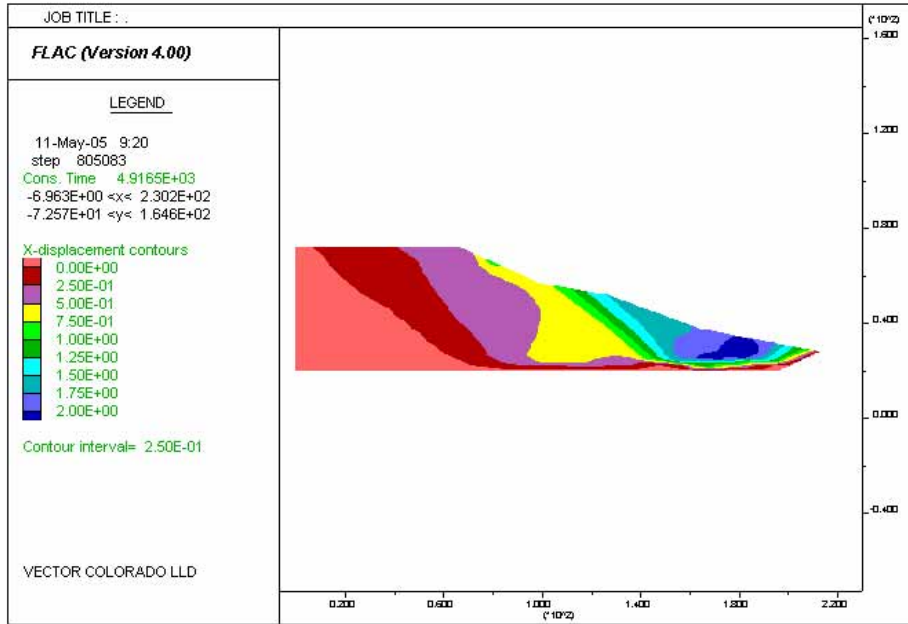


FIGURE B-2: Vertical Displacement Contours – Current geometry

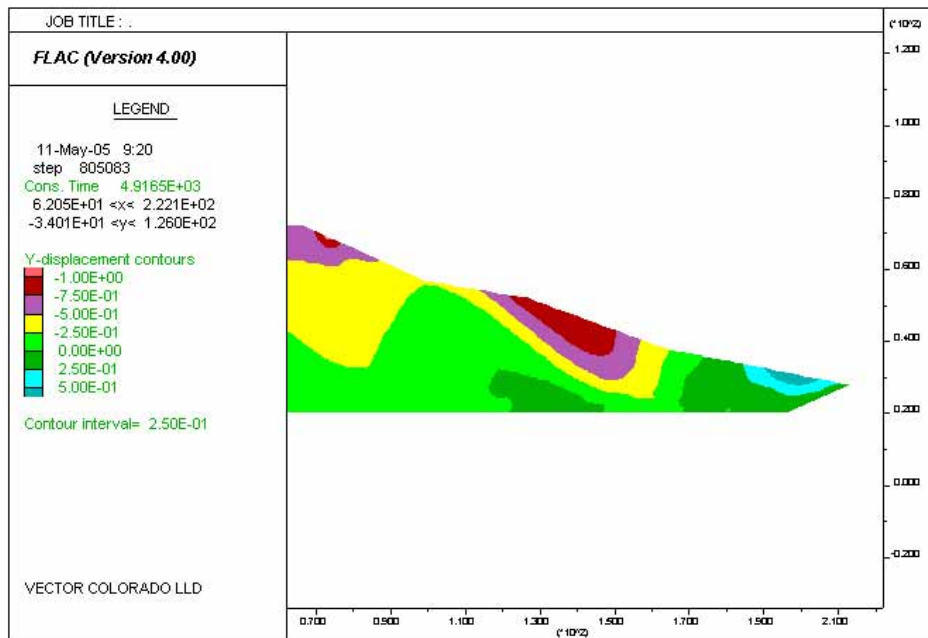


FIGURE B-3: Displacement (97 sec) – Current geometry

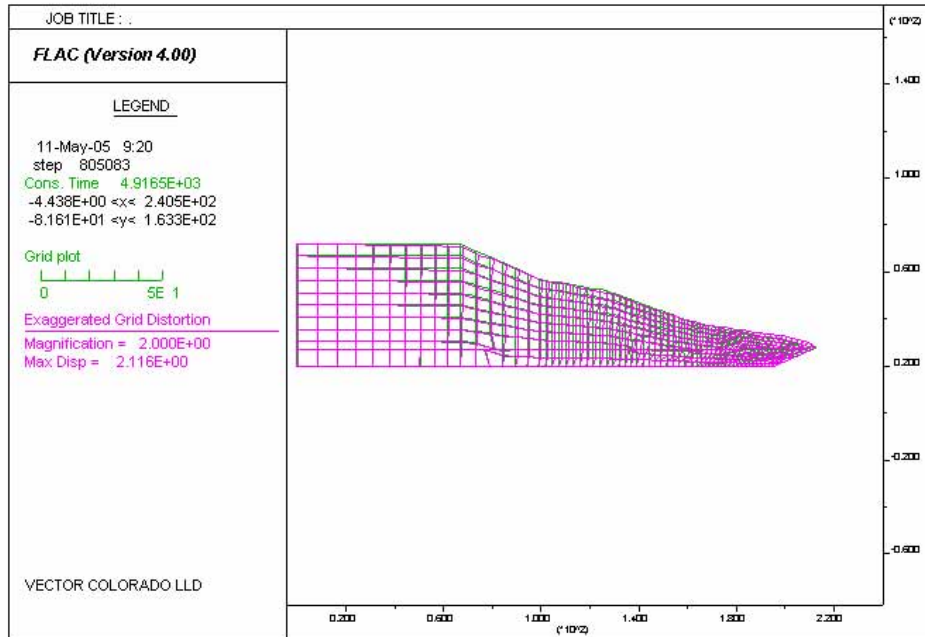


FIGURE B-4: Same as Fig B-3 – zoom – Current geometry

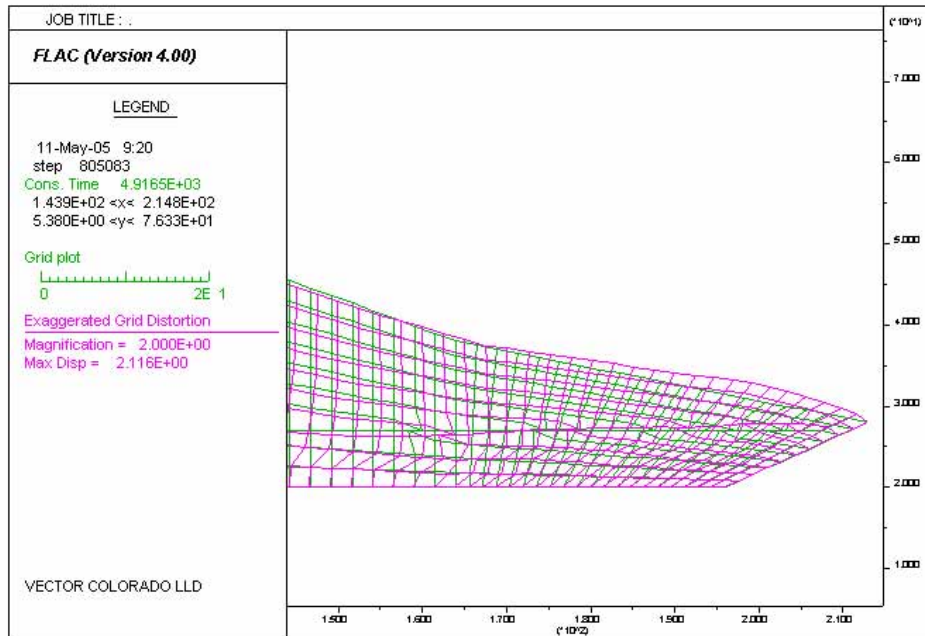


FIGURE B-5: Displacement  $S_u/p'=0.15$

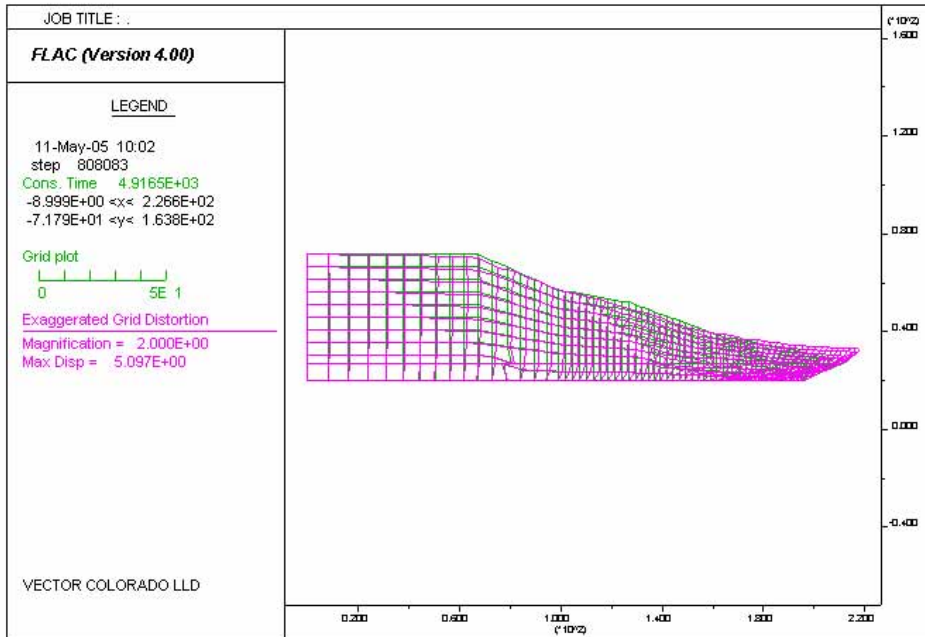
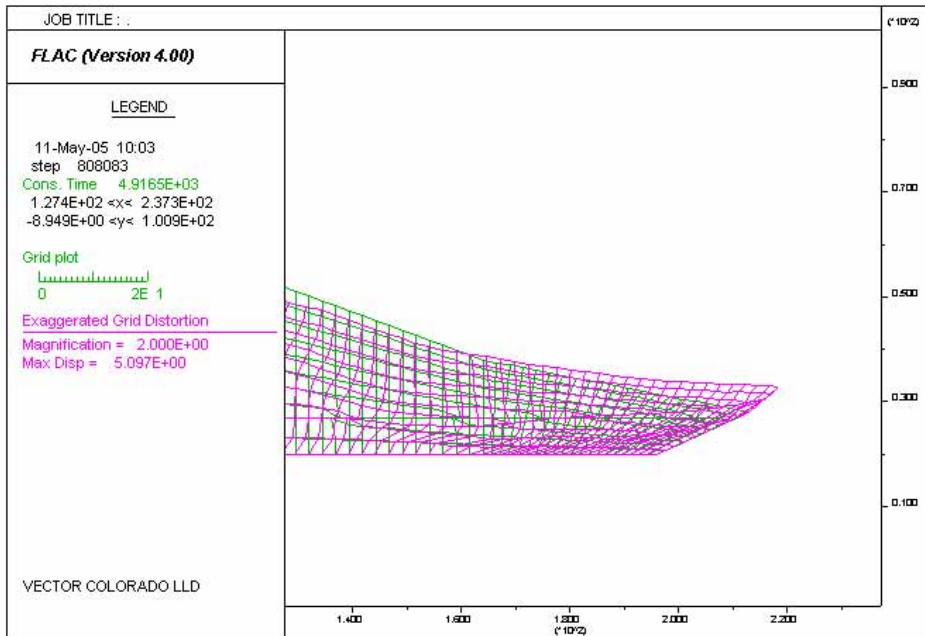


FIGURE B-6: Same as Figure B-5 – zoom – Current geometry



### APPENDIX C – 50 YEARS RETURN PERIOD

FIGURE C-1: Horizontal Displacement Contours – Current geometry

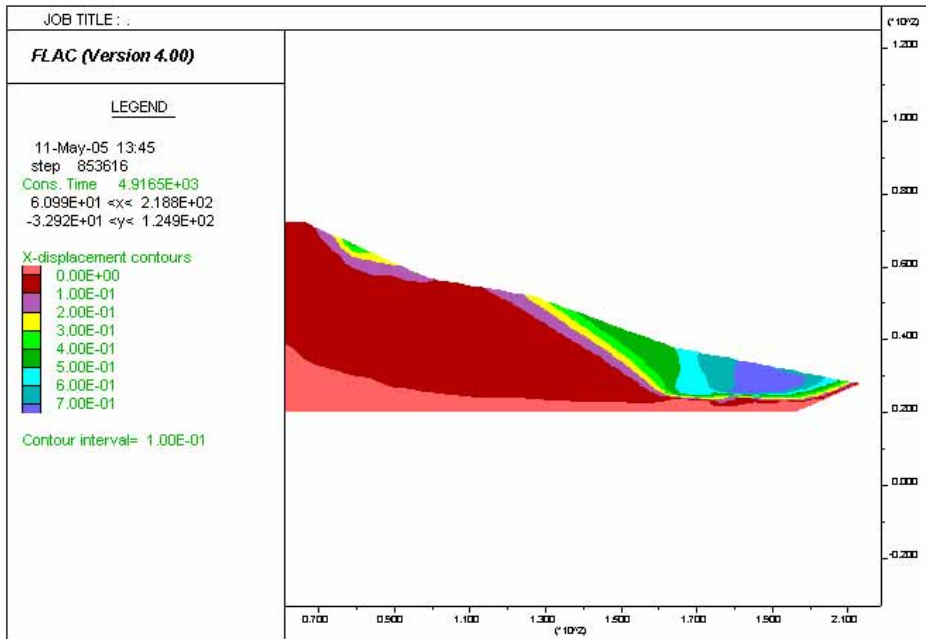


FIGURE C-2: Vertical Displacement Contours – Current geometry

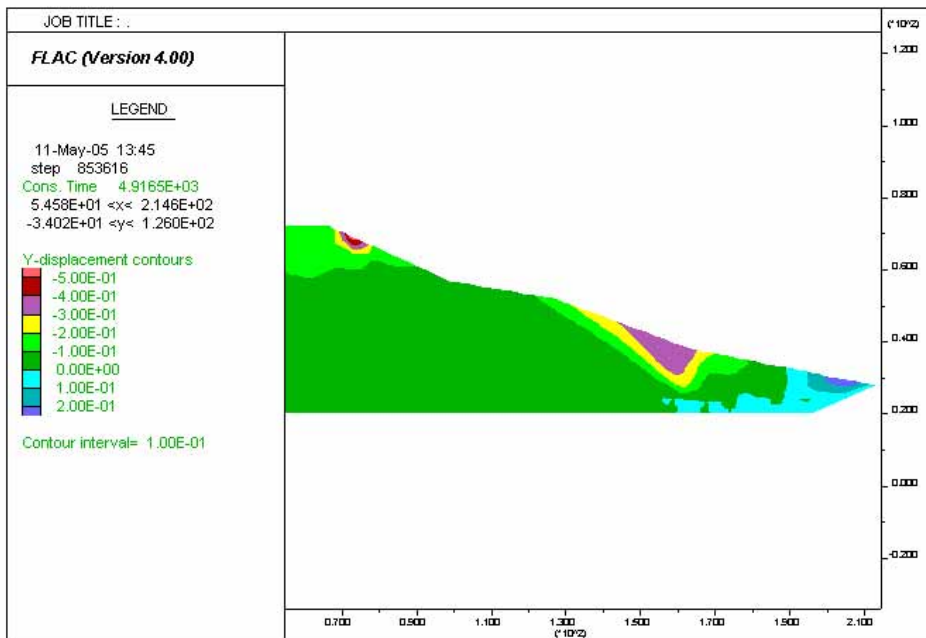


FIGURE C-3: Displacement (97 sec) – Current geometry

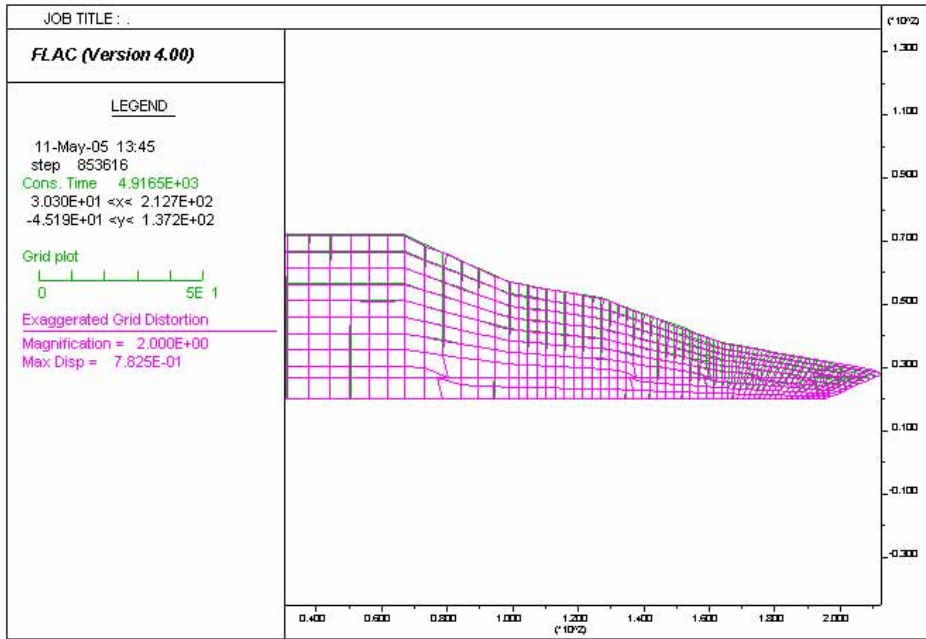


FIGURE C-4: Same as Fig C-3 – zoom – Current geometry

